Virologica Sinica 39 (2024) 600–608

Contents lists available at ScienceDirect

Virologica Sinica

journal homepage: www.keaipublishing.com/en/journals/virologica-sinica
www.virosin.org

Research Article

Identification of residues in Lassa virus glycoprotein 1 involved in receptor switch

Jiao Guo [a,c], Yi Wan [a,b], Yang Liu [a], Xiaoying Jia [a,b], Siqi Dong [a,b], Gengfu Xiao [a,b], Wei Wang [a,b,*]

[a] State Key Laboratory of Virology, Wuhan Institute of Virology, Center for Biosafety Mega-Science, Chinese Academy of Sciences, Wuhan 430071, China
[b] University of the Chinese Academy of Sciences, Beijing 100049, China
[c] The Xi'an Key Laboratory of Pathogenic Microorganism and Tumor Immunity, School of Basic Medicine, Xi'an Medical University, Xi'an 710021, China

ARTICLE INFO

Keywords:
Lassa virus (LASV)
Lysosome-associated membrane protein 1 (LAMP1)
Glycoprotein
Receptor switch
Membrane fusion

ABSTRACT

Lassa virus (LASV) is an enveloped, negative-sense RNA virus that causes Lassa hemorrhagic fever. Successful entry of LASV requires the viral glycoprotein 1 (GP1) to undergo a receptor switch from its primary receptor alpha-dystroglycan (α-DG) to its endosomal receptor lysosome-associated membrane protein 1 (LAMP1). A conserved histidine triad in LASV GP1 has been reported to be responsible for receptor switch. To test the hypothesis that other non-conserved residues also contribute to receptor switch, we constructed a series of mutant LASV GP1 proteins and tested them for binding to LAMP1. Four residues, L84, K88, L107, and H170, were identified as critical for receptor switch. Substituting any of the four residues with the corresponding lymphocytic choriomeningitis virus (LCMV) residue (L84 N, K88E, L10F, and H170S) reduced the binding affinity of LASV GP1 for LAMP1. Moreover, all mutations caused decreases in glycoprotein precursor (GPC)-mediated membrane fusion at both pH 4.5 and 5.2. The infectivity of pseudotyped viruses bearing either GPC^{L84N} or GPC^{K88E} decreased sharply in multiple cell types, while L107F and H170S had only mild effects on infectivity. Using biolayer light interferometry assay, we found that all four mutants had decreased binding affinity to LAMP1, in the order of binding affinity being L84 N > L107F > K88E > H170S. The four amino acid loci identified for the first time in this study have important reference significance for the in-depth investigation of the mechanism of receptor switching and immune escape of LASV occurrence and the development of reserve anti-LASV infection drugs.

1. Introduction

Lassa virus (LASV) belongs to the *Arenaviridae* family of enveloped, negative-sense, bi-segmented RNA viruses and is classified as an Old World (OW) mammarenavirus (Radoshitzky et al., 2015). It is transmitted from the rodent host *Mastomys natalenis* to humans via contaminated excreta (Goeijenbier et al., 2013). LASV infections cause Lassa hemorrhagic fever, which causes high mortality in hospitalized patients. However, there are no FDA-approved vaccines or specific antiviral agents against LASV (Yun and Walker, 2012).

The LASV RNA genome encodes an RNA-dependent RNA polymerase (L), nucleoprotein (NP), matrix protein (Z), and a highly glycosylated membrane glycoprotein (GP). GPC is synthesized as an inactive precursor glycoprotein complex, then cleaved into three subunits: a stable signal peptide (SSP), a receptor-binding subunit (GP1), and a membrane-spanning fusion subunit (GP2) (Wang W. et al., 2016). During cellular entry, LASV GP1 interacts with the primary receptor, alpha-dystroglycan (α-DG), on the plasma membrane; LASV is then internalized through macropinocytosis, subsequently reaching the late endosomal compartment (Oppliger et al., 2016). In this low pH environment, GP undergoes irreversible structural changes that decrease its affinity for α-DG, while increasing its affinity for the acidic receptor, lysosome-associated membrane protein 1 (LAMP1) (Nunberg and York, 2012; Jae et al., 2014; Cohen-Dvashi et al., 2016; Oppliger et al., 2016). A histidine triad (H92/93/230) in $GP1_{LASV}$ is highly conserved among OW mammarenaviruses and is essential for LAMP1 binding (Cohen-Dvashi et al., 2015). Several other residues in LASV GP1 that are not shared by other OW mammarenaviruses have also been reported to be critical for LAMP1 binding (Israeli et al., 2017).

Here, we compared LASV with the prototypical OW mammarenavirus, lymphocytic choriomeningitis virus (LCMV), which is genetically and serologically similar to LASV but does not interact with LAMP1. We mutated several residues in $GP1_{LASV}$ to their corresponding residues in $GP1_{LCMV}$, tested its ability to bind to LAMP1, and found four residues involved in LAMP1 binding.

* Corresponding author.
E-mail address: wangwei@wh.iov.cn (W. Wang).

https://doi.org/10.1016/j.virs.2024.06.001
Received 18 January 2024; Accepted 31 May 2024
Available online 6 June 2024

2. Materials and methods

2.1. Cell lines, plasmids, and antibodies

HEK293T (ATCC Number: CRL-3216), BHK (ATCC Number: CCL-10), A549 (ATCC Number: CCL-185), and Vero cells (ATCC Number: CRL-1586) were maintained in Dulbecco's modified Eagle's medium (DMEM; Gibco, Grand Island, NY, USA) supplemented with 10% fetal bovine serum (FBS; Gibco, Grand Island, NY, USA). 293F cells were cultured in Freestyle 293 expression medium (Invitrogen, Carlsbad, CA, USA). GPC_{LASV} (Josiah strain, GenBank HQ688673.1) was synthesized by Sangon Biotech (Shanghai, China) and subcloned into the pCAGGS vector. The recombinant pcDNA3.1-$GP1_{LASV}$-Fc plasmid was constructed by inserting codon-optimized $GP1_{LASV}$, which was synthesized de novo by GenScript (Nanjing, China). Distal LAMP1-Fc expressing plasmid was a gift from Professor Ron Diskin (Department of Structural Biology, Weizmann Institute of Science, Rehovot, Israel).

Anti-LAMP1 antibody was purchased from Millipore (Billerica, MA, USA). Anti-GAPDH, anti-α-tubulin, anti-Fc, and horseradish peroxidase (HRP)-conjugated secondary antibodies were obtained from Proteintech (Wuhan, China). Anti-$GP2_{LASV}$ antibodies were produced in our laboratory (Wang P. et al., 2018; Liu et al., 2021).

2.2. Protein expression and purification

$GP1_{LASV}$-Fc and distal LAMP1-Fc were transfected into HEK 293F cells using polyethylenimine (PEI) at a density of 2.0×10^6/mL. Overgrowth of the cells was controlled by adding 2 mmol/L sodium valproate and shaking at 120 rpm with 8% CO_2 at 37 °C. After 5 days, suspension cultures were harvested, centrifuged at 3500×*g* for 15 min, and sterilized by passage through 0.45 μm filters (Thermo Scientific, USA). Secreted proteins were purified from the culture supernatants using a protein A + G affinity column (GE Healthcare) according to the manufacturer's instructions. Protein concentrations were determined based on absorption at 280 nm (UV_{280}) using theoretical extinction coefficients. Protein samples were analyzed using blue native polyacrylamide gel electrophoresis (PAGE) and stained with Coomassie blue to assess purity.

2.3. LAMP1 pulldown assays

Assays were performed as described previously (Cohen-Dvashi et al., 2016; Israeli et al., 2017). Briefly, LASV GP1-Fc protein was incubated overnight with protein A + G Sepharose beads (ProteinTech) at 4 °C and then washed five times with NETI buffer (50 mmol/L Tris-HCl, 1 mmol/L EDTA, 150 mmol/L sodium chloride, 0.5% [vol/vol] IGEPAL, pH 8.0). The beads were incubated with extracts from HEK 293T cells prepared in NETI buffer and adjusted to pH 5.0, at 4 °C for 3 h. Proteins were eluted using 20 mmol/L Tris-HCl (pH 8.0) and 150 mmol/L sodium chloride and precipitated using cold acetone at −20 °C. Protein pellets were recovered in sample buffer and subjected to western blotting.

2.4. Western blot analysis

Samples containing equal amounts of protein were separated using sodium dodecyl sulfate (SDS)-PAGE and then transferred to polyvinylidene difluoride (PVDF) membranes (Millipore). After blocking with 5% skim milk in TBST for 2 h, membranes were incubated with primary antibodies (diluted 1:1000) for 1 h, followed by incubation with horseradish peroxidase (HRP)-conjugated secondary antibodies (diluted 1:2000; ProteinTech) for 45 min. Membranes were gently soaked in an enhanced chemiluminescence (ECL) solution (Millipore) and protein bands were visualized using a ChemiDoc MP gel imager (Bio-Rad Laboratories, Hercules, CA, USA).

2.5. Membrane fusion assay

293T cells were pre-seeded in 24-well plates pre-coated with poly-D-lysine (Sigma). Seeded cells were co-transfected with pEGFP-N1 and pCAGGS-LASV GPC plasmids using PEI. After 24 h of transfection, cells were incubated in different pH medium for 15 min at 37 °C to enable glycoprotein triggering, respectively. The cells were then restored to neutral medium and cultured for an additional 4 h to allow membrane rearrangement. Syncytium formation was manually identified and visualized using a fluorescence microscope (Olympus).

To quantify the efficiency of membrane fusion, a dual-luciferase reporter assay was performed as described previously (Wang et al., 2018; Cao et al., 2021; Liu et al., 2021). Briefly, 293T cells in a 24-well plate were co-transfected with plasmids expressing T7 RNA polymerase (pCAGT7) and pCAGGS-LASV GPC. 293T cells in a 6-well plate were transfected with pRL-CMV together with pT7EMCVLuc CMV (the three plasmids used in this reporter assay were kindly gifted by Yoshiharu Matsuura, Osaka University, Osaka, Japan). After transfection for 24 h, the cells were gently trypsinized and co-cultured for 6 h in DMEM containing 10% FBS. Membrane fusion was initiated by treatment with acidified medium, which was adjusted using citric acid buffer, and incubated in DMEM supplemented with 2% FBS for 24 h. Membrane fusion activity was quantitatively assessed by detecting the expression of firefly luciferase and sea pansy luciferase using the Dual-Luciferase Reporter Assay System (Promega, Madison, WI, USA) according to the manufacturer's protocol.

2.6. Production of pseudovirus

Plasmid pVSVΔG-eGFP (Addgene plasmid #31842) was modified to pVSVΔG-Rluc to generate LASV GPC pseudotyped viruses (LASVpv). LASVpv were produced as described previously (Wang et al., 2018; Cao et al., 2021; Liu et al., 2021; Zhu et al., 2021). Briefly, 293T cells were transfected with the envelope LASV GPC-pCAGGS plasmid or its mutant derivatives using PEI. After 24 h, the cells were infected with pVSVΔG-Rluc at an MOI of 0.1, for 1 h. Culture supernatants containing viral particles were harvested 30 h later and centrifuged to remove cell debris.

Viral RNA was extracted from 200 μL of pseudovirus using the MiniBEST Viral RNA/DNA Extraction Kit Ver.5.0 (TaKaRa, Japan), and the extracted mRNA was used as a template for reverse transcription using M-MLV reverse transcriptase (Promega, Madison, WI, USA). Virus was quantified using real-time PCR using SYBR Premix Ex Taq™ (Applied Biosystems, Thermo Fisher Scientific, USA) according to the manufacturer's instructions. Ten-fold serial dilutions of VSV-eGFP were used to construct a standard curve for calculating viral copy numbers.

2.7. Construction of LAMP1-knockout A549 cells

LAMP1-knockout A549 cells were constructed using the CRISPR/Cas9 system. The primers covering the cleavage site on both strands were as follows: forward primer, CACCGAACGGGACCGCGTGCATAA and reserve primer, AAACTTATGCACGCGGTCCCGTTC. A549 cells (5×10^5) were seeded into one well of a six-well plate and were transfected with 600 ng of plasmid with 5 μL of Lipofectamine (2000) (Invitrogen) in 200 μL of OptiMEM (Gibco). At 48 h post transfection, fresh medium containing 2 μg/mL puromycin was added, and the cells were incubated for 2 days. Puromycin-resistant A549 cells were then diluted and cloned. Finally, single-cell clones were identified, amplified, genotyped, and cultured for further experiments. LAMP1 expression in the knockout line was evaluated using Western blotting with an anti-LAMP1 antibody.

2.8. Infectivity assay

To measure the effect of LAMP1 knockout on the infectivity of wild-type and mutant LASVpv, BHK, HEK 293T, and Vero cells, as well as

wild-type and KO-LAMP1 A549 cells were seeded at a density of 1.5×10^5/mL into 96-well plates and then infected 16 h later with the indicated virus (2×10^6 viral copy number). Supernatants were removed at 24 h p.i., and cell lysates were collected to perform luciferase assays.

2.9. Kinetics assay by biolayer interferometry (BLI) assay

The distal LAMP1-Fc fusion protein was biotinylated in a buffer containing 50 mmol/L sodium citrate (pH 5.0) and 0.02% Tween. The interaction between distal-LAMP1 protein and $GP1_{LASV}$ was assessed using BLI on an Octet RED96 instrument (Pall ForteBio LLC, CA). Biotinylated distal LAMP1 (50 μg/mL) was immobilized on the streptavidin-coated biosensors, then four concentrations (2-fold dilutions; 200–1600 nmol/L) of $GP1_{LASV}$-Fc protein were used for detection. The experiments consisted of five steps: baseline acquisition, distal LAMP1 protein loading onto the sensor, second baseline acquisition, association of $GP1_{LASV}$ protein, and dissociation of $GP1_{LASV}$ protein. The baseline and dissociation steps were assessed using kinetic buffer. The ability of $GP1_{LASV}$ to bind to LAMP1 was determined using response value measurements (Thomson et al., 2021). Experimental data were analyzed using Octet data acquisition software v.7.1, and curve fitting was performed using GraphPad prism (Kumar and Sarkar, 2019).

2.10. IIH6 inhibition assay

To determine whether the four identified residues affect LASV binding to the cell surface receptor, A549 cells were pretreated with IIH6 (sc-53987; Santa Cruz Biotechnology, Dallas, TX, USA) or control IgM (sc-53347; Santa Cruz Biotechnology) at 4 °C for 2 h (Moraz et al., 2013; Oppliger et al., 2016). The presence of functionally glycosylated α-DG was detected by MAb IIH6, which recognizes the LARGE-derived sugar polymers implicated in virus and ECM binding. The cells were then incubated in ice and wild type and mutant LASVpv were added for 1 h, respectively. After three washes with phosphate-buffered saline (PBS), the cells were then incubated at 37 °C for 24 h. Luciferase activity were quantitatively evaluated 24 h later as described above.

2.11. Statistical analysis

Statistical analysis were performed using GraphPad Prism 7 software (GraphPad Inc., La Jolla, CA, USA). All statistical analyses were performed using Student's *t*-test.

3. Results

3.1. Four single-residue substitutions in $GP1_{LASV}$ disrupt LAMP1 binding

To investigate the basis for the differential use of LAMP1 by LASV and LCMV (Fig. 1A and B), we examined the amino acid sequences of $GP1_{LASV}$ and $GP1_{LCMV}$ to identify non-conserved residues: i) spatially located at the interface of $GP1_{LASV}$ and LAMP1, ii) spatially located in proximity of the histidine triad (H92/93/230), and iii) those altering polar amino acids. These amino acids were selected and mutated to the corresponding residue in $GP1_{LCMV}$. LAMP1 binding was evaluated using pull-down assays at pH 5.0. As shown in Fig. 1C and D, four mutants, L84 N, K88E, L107F, and H170S, disrupted the binding of $GP1_{LASV}$-Fc to LAMP1; whereas other mutants, such as E100S, T101S, K116 N, H124L, K125 N and Q232R, had little effect. H92Y, H93Y, and H230Y were used as the positive controls, none of which showed binding to LAMP1, consistent with the previous reports (Cohen-Dvashi et al., 2015, 2016).

3.2. Effects of the mutations on GPC cleavage efficiency

To evaluate the effect of the four mutations on the cleavage processing of LASV GPC into GP1 and GP2, 293T cells were transfected with pCAGGS vectors encoding wild-type (WT) and the mutant GPCs. As shown in Fig. 2, GPC^{L107F} and GPC^{H170S} exhibited similar cleavage efficiency to that of GPC^{WT}, whereas GPC^{L84N} and GPC^{K88E} showed cleavage processing defects (Fig. 2A). Compared with GPC^{WT}, the cleavage efficiency of GPC^{L84N} decreased to only approximately 4% of that of GPC^{WT}. The cleavage efficiency of GPC^{K88E} was approximately 25% that of GPC^{WT} (Fig. 2B). There were no significant differences in the cleavage efficiencies of GPC^{L107F}, GPC^{H170S}, and GPC^{WT}, indicating that unlike L84 N and K88E, L107F and H170S might have little effect on the cleavage efficiency of GPC.

3.3. Effects of mutations on GPC-mediated membrane fusion

GPC cleavage is upstream of GPC-mediated membrane fusion, so a decrease in cleavage efficiency would lead to a reduction in the fusion activity. To this end, the effects of the substitutions on GPC-mediated membrane fusion were also tested. As shown in Fig. 3, the efficiency of membrane fusion mediated by GPC^{L84N} was lower than that of GPC^{WT} (<20%) at all tested pH values (4.5, 5.0, and 5.2). Compared with GPC^{WT}, the membrane fusion efficiency of GPC^{K88E} ranged from 42% to 63%, while that of GPC^{L107F} ranged from 46% to 80%. The decrease in fusogenicity of L84 N and K88E might be due to a deficiency in GPC cleavage. Notably, the membrane fusion efficiency of GPC^{H170S} was nearly twice as high as that of GPC^{WT} at pH 5.0. However, the membrane fusion efficiency of GPC^{H170S} was lower than that of GPC^{WT} at both pH 4.5 and pH 5.2, suggesting that pH 5.0 might be an optimal pH for GPC^{H170S}- mediated membrane fusion.

3.4. Four substitutions in $GP1_{LASV}$ reduce LASV infectivity

We constructed LASV pseudotyped viruses (PVs) with a VSV backbone and luciferase reporter gene. The genome copy numbers of $LASV_{PV}{}^{WT}$, $LASV_{PV}{}^{L84N}$, $LASV_{PV}{}^{K88E}$, $LASV_{PV}{}^{L107F}$, and $LASV_{PV}{}^{H170S}$ were 8.10×10^9, 2.05×10^9, 1.90×10^{10}, 1.18×10^{10}, and 7.88×10^9 per mL, respectively.

The WT and mutant viruses with the same copy number were used to infect different cell lines, and relative luminescence was measured to evaluate efficiency. In A549 and BHK cells, L84 N, K88E, L107F, and H170S significantly reduced infectivity relative to WT (Fig. 4). The infection efficiency of L84 N was reduced by 3.3 log values. In HEK 293T cells, L84 N and K88E significantly reduced infectivity, whereas L107F and H170S had little effect. In Vero cells, the infectivity of L84 N, K88E, and H170S was significantly reduced, whereas L107F had little effect. In summary, the infectivity of GPC^{L84N} and GPC^{K88E} mutant PVs was sharply decreased in HEK 293T and Vero cell lines, whereas L107F and H170S had milder effects on infectivity (Fig. 4).

To assess the role of LAMP1 in LASV infection, we knocked out LAMP1 in A549 cells using CRISPR/Cas9 gene editing, and then measured LAMP1 expression using a Western blotting assay (Fig. 5A). $LASV_{PV}$ replication was reduced in LAMP1-knockout A549 cells compared to wild-type A549 cells, and LAMP1 transcomplementation restored the infectivity of pseudotyped viruses in LAMP1 knockout (KO) A549 cells (Fig. 5B). Moreover, all four mutants exhibited a smaller decrease of infectivity in LAMP1 KO cells compared to the decrease shown with $LASV_{PV}^{WT}$ in KO cells. This indicated that LAMP1 knockout exerted a lesser impact on mutant viruses, suggesting the importance of these four residues in binding to LAMP1.

3.5. GP1 mutants have reduced binding affinity for LAMP1

To further evaluate the role of the mutated residues (L84 N, K88E, L107F, and H170S) in LAMP1 binding, biolayer interferometry (BLI) assay was performed to test the ability of these mutants to bind to LAMP1 (Thomson et al., 2021). As shown in Fig. 6, the WT GP1-Fc as well as the entire mutant GP1-Fc exhibited dose-dependent binding to LAMP1, while LCMV GP1-Fc showed no binding. Specifically, the relative LAMP1 binding affinities were L84 N > L107F > K88E > H170S (Fig. 6A and B).

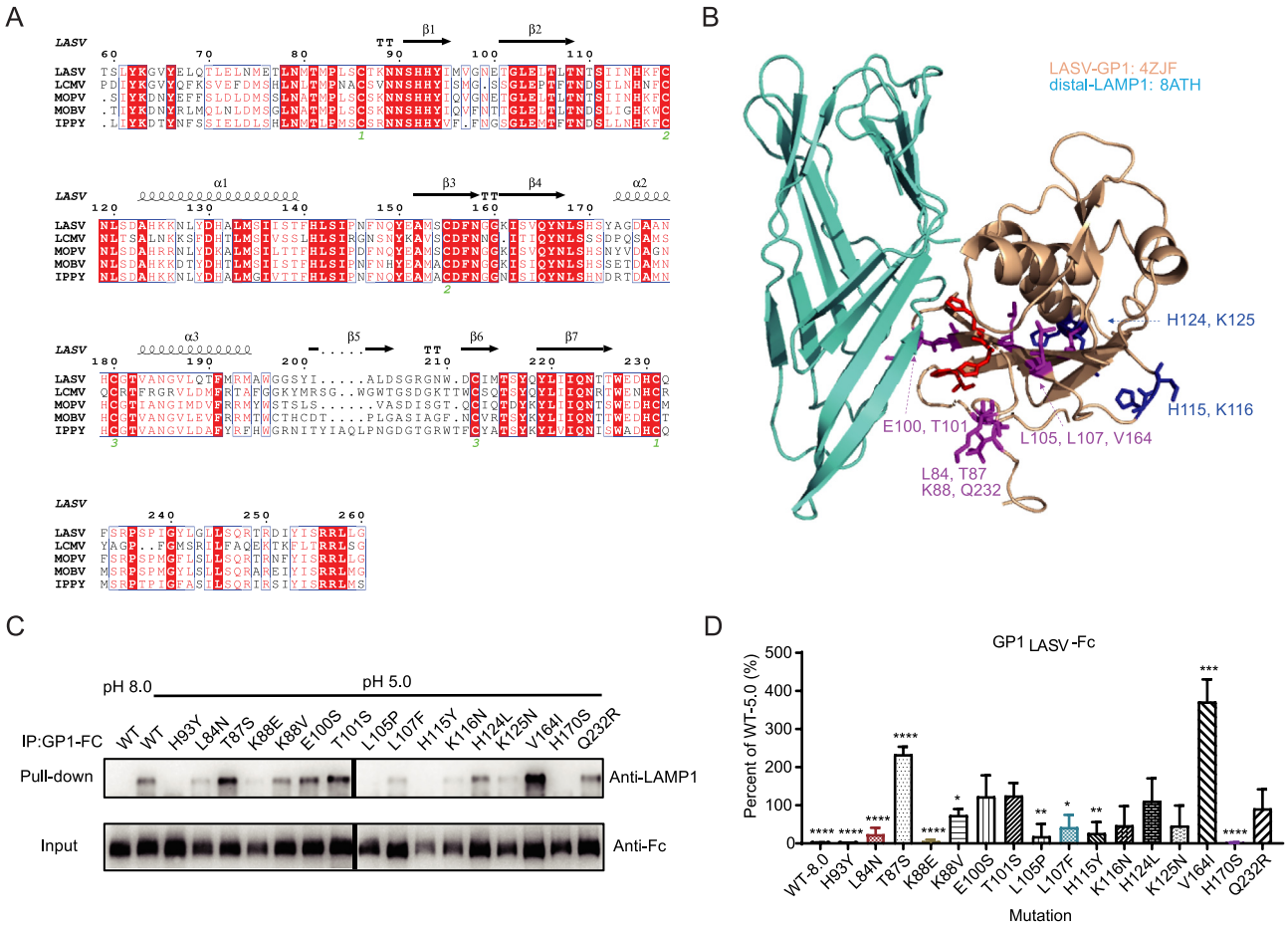

Fig. 1. Binding ability of the mutant $GP1_{LASV}$ to LAMP1. **A** Multiple sequence alignment of GP1 proteins of representative Old World mammarenaviruses. The UniProt accession codes of the sequences are P08669 (LASV), P07399 (LCMV), P19240 (MOPV), Q2A069 (MOBV), and Q27YE4 (Ippy virus, IPPYV). Fully conserved residues were highlighted with a red background, and partially conserved residues were presented in red. The secondary structure observed with $GP1_{LASV}$ (PDB: 4ZJF) was indicated above the sequence, and cysteine involved in the disulfide bond was numbered below the alignment in green. This graphical representation was generated using ESPript (http://espript.ibcp.fr). **B** Ribbon diagram of the LASV-GP1/distal-LAMP1 complex. The crystal structure of LASV-GP1 (PDB no. 4ZJF) and distal-LAMP1 (PDB no. 8ATH) was used to build the complex using the ZDOCK 3.0.2 program. Residues located in the interface of LASV-GP1 and LAMP1, and residues located spatially close to the histidine triad (H92/93/230) are colored magentas. Polar amino acids which were not conserved between LASV and LCMV are colored blue. The histidine triad are colored red. **C** Images of LAMP1 pull-down assays by wild-type (WT) and mutated $GP1_{LASV}$-Fc. $GP1_{LASV}$-Fc was immobilized on sepharose beads, incubated with equal amount of cell lysates at pH 5.0 and pH 8.0, pulled down, and eluted. Protein pellets were recovered and subjected to Western blot analysis. **D** Quantitative analysis of the pull-down efficiencies based on the intensity of the bands. Data were presented as means ± SDs from three independent experiments. ****$P < 0.0001$, ***$P < 0.001$, **$P < 0.01$, *$P < 0.05$.

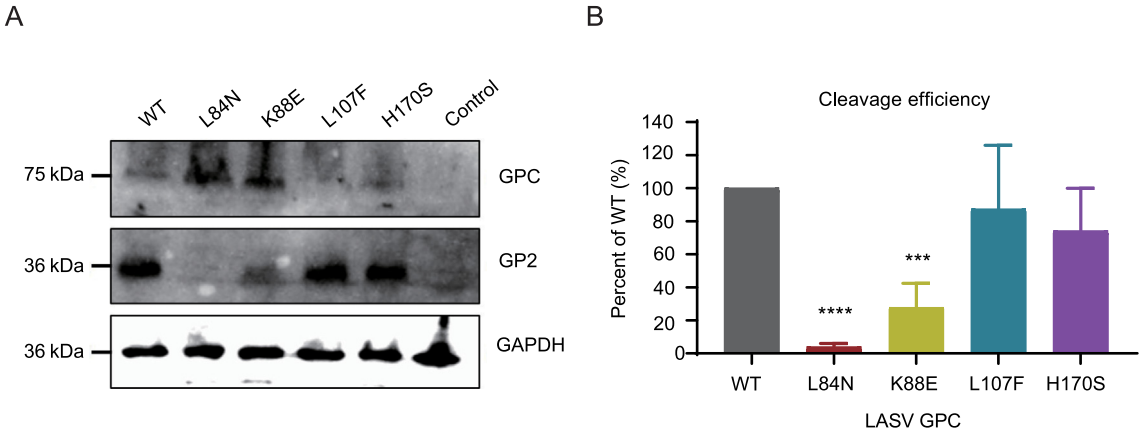

Fig. 2. Cleavage processing of wild-type (WT) and mutant LASV GPCs. **A** 293T cells were transfected with WT or one of the four GPC mutants (L84 N, K88E, L107F, and H170S). The equal cell lysates were subjected to Western blotting and probed with an anti-LASV GP2 antibody. The image was representative of three independent experiments. **B** Quantitative analysis of the cleavage efficiencies based on the intensity of the bands. Data were presented as means ± SDs from three independent experiments. ****$P < 0.0001$, ***$P < 0.001$.

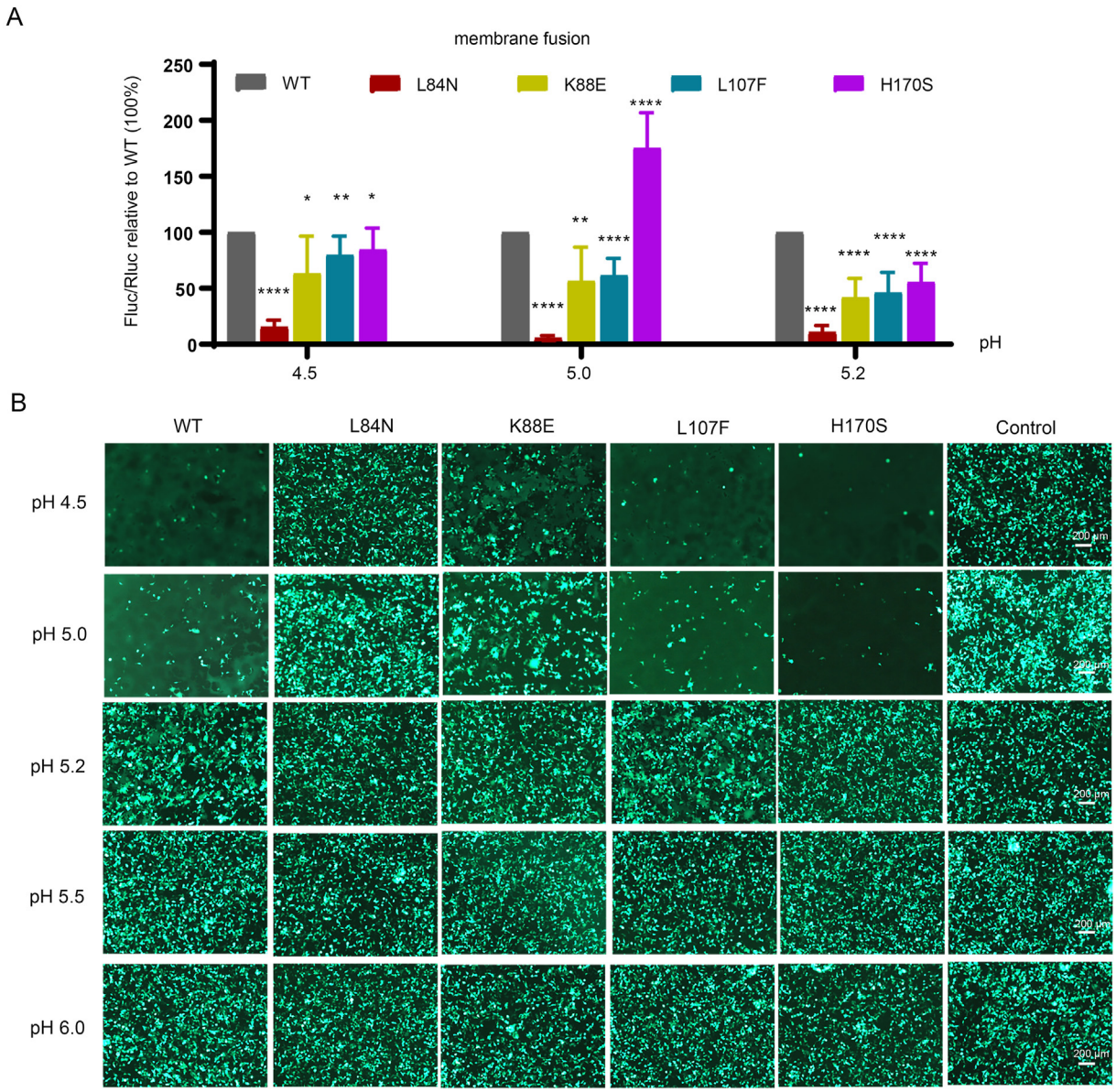

Fig. 3. Membrane fusion by wild-type (WT) and four mutant GPCs. **A** Quantification of membrane fusion using a dual-luciferase reporter assay at the indicated pH values. Data are presented as means ± SDs from three independent experiments. ****$P < 0.0001$, ***$P < 0.001$, **$P < 0.01$, *$P < 0.05$. **B** Qualitative analysis of membrane fusion was performed in 293T cells co-transfected with pEGFP-N1 and pCAGGS-LASV GPC plasmids. Scale bar, 200 μm.

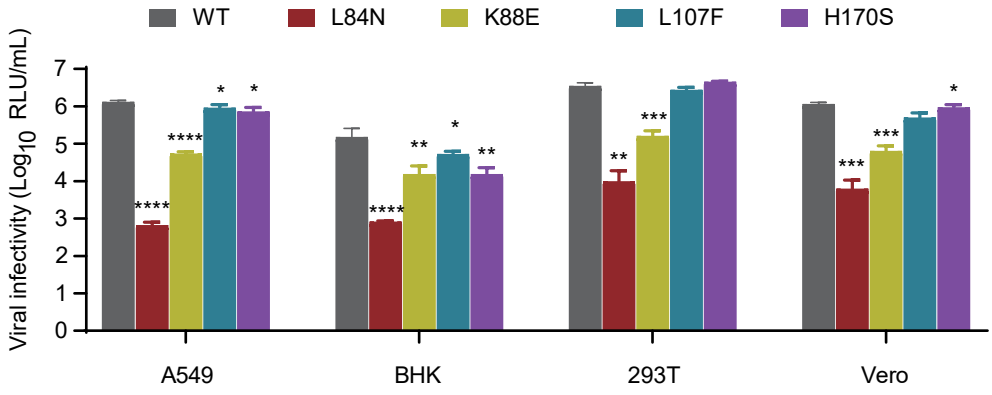

Fig. 4. Infectivity of multiple cell lines by the mutant pseudoviruses. Viral copy number was normalized using quantitative RT-PCR. After normalization, A549, BHK, 293T, and Vero cells in 96-wells plate were infected with 2×10^6 copies/well, respectively. After 24 h, the cell lysates were subjected to evaluate the *Renilla* luciferase activities. Data were presented as means ± SDs from three independent experiments. ****$P < 0.0001$, ***$P < 0.001$, **$P < 0.01$, *$P < 0.05$.

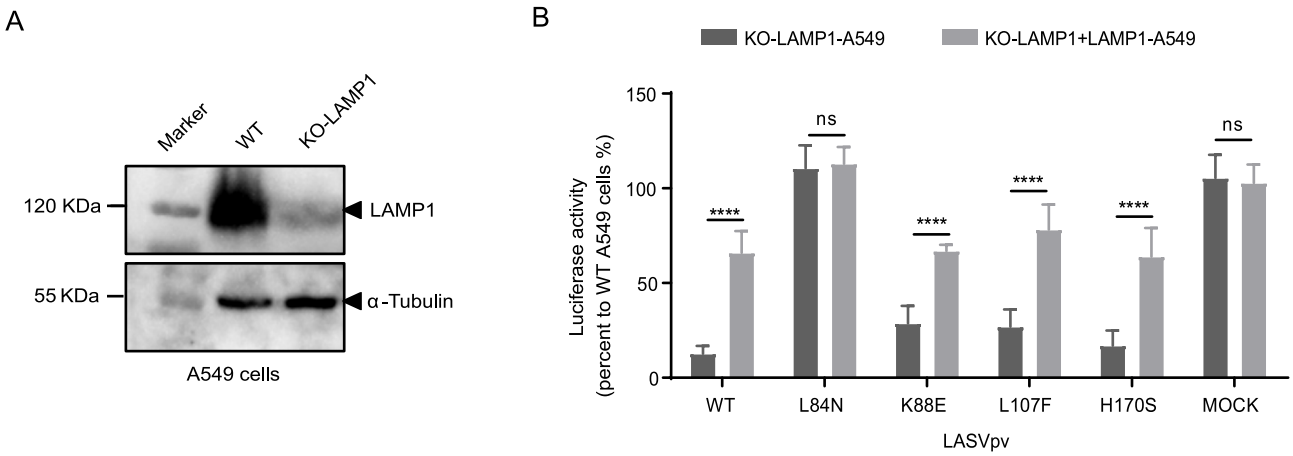

Fig. 5. Infectivity of pseudoviruses on LAMP1-knockout (KO) and LAMP1 replacement A549 cells. **A** wild-type (WT) and LAMP1-KO A549 cells were analyzed using Western blotting with antibody against LAMP1. **B** LASVpv^{WT}, LASVpv^{L84N}, LASVpv^{K88E}, LASVpv^{L107F}, and LASVpv^{H170S} infected LAMP1-knockout and LAMP1 replacement cells, respectively, the mock group is a blank control group, and the cells were lysed and assayed for RLU at 24 h post-infection. Data are presented as means ± SDs from three independent experiments. ****$P < 0.0001$; ns, not significant.

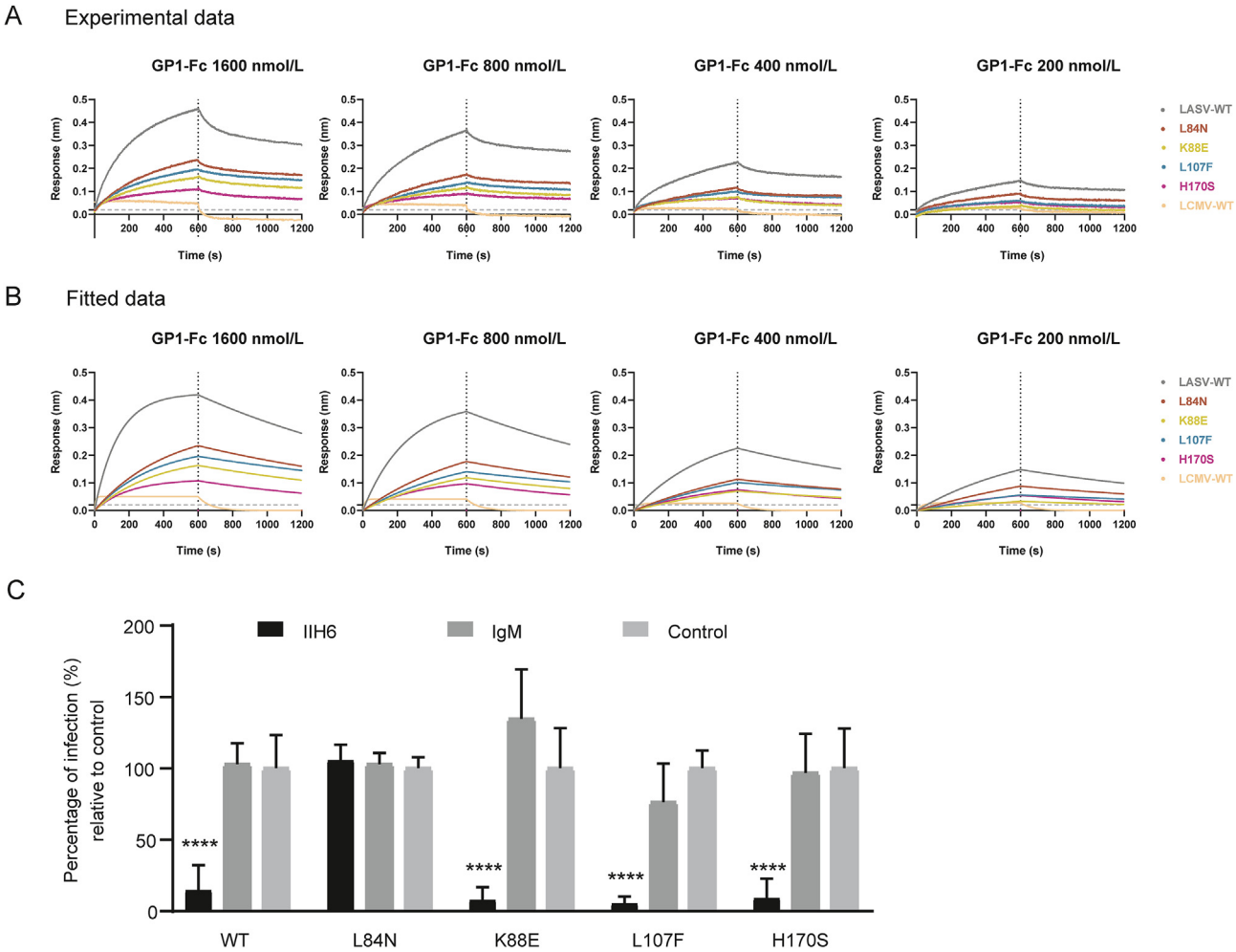

Fig. 6. Analysis of GP1-LAMP1 interaction. **A, B** Binding of wild-type (WT) and mutant GP1$_{LASV}$ to the distal domain of LAMP1 was measured using the Octet RED 96 instrument. Each column presents the maximum values of the binding curves. The response values (nm) to the indicated concentrations of GP1$_{LASV}$ (1600, 800, 400, and 200 nmol/L) were measured. Experimental data are shown in (**A**); these data were fit with a 1:1 global fitting model and the fitted curves are presented in (**B**). **C** IIH6 inhibition assay was performed to investigate the effects of GP1 mutants on LASVpv binding. A549 cells were incubated with 200 μg/mL IIH6 or IgM control at 37 °C for 1 h. LASVpv$_{WT}$ and mutant LASVpv were added and treated at 4 °C for 1 h. The unbound virus particles were washed for three times with cold PBS. After 24 h, cells were lysed and luciferase activity was measured using the Rluc assay system. The results are the mean of three independent determinations. Data are presented as means ± SDs from three independent experiments. ****$P < 0.0001$.

LAMP1 binding was robustly abolished by the H170S substitution; the K88E, L84 N, and L107F mutants weakly bound to LAMP1. These results are consistent with those of the LAMP1 pulldown assay, indicating that L84 N, K88E, L107F, and H170S have negative effects on LAMP1 binding.

Furthermore, we performed an IIH6 inhibition assay to explore the effects of GP1 mutants on LASVpv binding. As shown in Fig. 6C, IIH6 significantly block $LASV_{PV}^{WT}$, $LASV_{PV}^{K88E}$, $LASV_{PV}^{L107F}$, and $LASV_{PV}^{H170S}$ transduction to the cell, suggesting that GP1 mutants have little effect on the binding of LASV GP1 to the cell surface receptor.

4. Discussion

LASV GPC mediates viral entry into host cells; therefore, substantial efforts have been made to understand its structure, function, and immunobiology (Enria et al., 1984; Sanchez et al., 1989). Successful LASV entry requires a switch in binding from α-DG to the endosomal receptor LAMP1 (Jae et al., 2014). Ebola virus (EBOV) uses a similar, multistep entry strategy, employing Niemann-Pick type C1 (NPC1) to complete its entry step (Carette et al., 2011; Jae and Brummelkamp, 2015; Wang H. et al., 2016). Tetraspanin CD63 was shown to enhance the efficiency of GP-mediated membrane fusion for another OW mammarenavirus Lujo virus (LUJV), and is hypothesized to be a possible second receptor for LUJV entry (Raaben et al., 2017; Cohen-Dvashi et al., 2018).

The prototypical OW mammarenavirus LCMV is genetically and serologically similar to LASV and also is pathogenic to humans; both share similar receptor-binding domains involved in α-DG binding (Acciani et al., 2017). A previous study implicated a conserved, positively charged histidine triad (H92/93/230) in $GP1_{LASV}$ binding to LAMP1 (Cohen-Dvashi et al., 2015), located on the β-sheet face of $GP1_{LASV}$. $GP1_{LCMV}$ shares this histidine triad, but LCMV does not undergo receptor switch. The GP1 sequence is different between the two, which might lead to differences in receptor binding.

A previous study implicated important fragments in addition to the histidine triad in LASV receptor switch. These residues were mainly located in β5 and L7 of GP1 domain from the Morogoro virus (MORV) and play key roles in LAMP1 binding. Notably, when partial fragments of $GP1_{MORV}$ were mutated to their corresponding LASV residues, the resulting chimeric $GP1_{MORV}$ could bind to LAMP1, suggesting that these residues play a key role in the binding of $GP1_{LASV}$ to LAMP1 (Israeli et al., 2017). Exploring the biological functions of the key sites on LASV GP1 will help elucidate the mechanism of LASV infection and provide strategies for the development of attenuated vaccines against LASV infection.

Based on the crystal structure of $GP1_{LASV}$ (PDB: 5VK2), K88 is located in the center of the histidine triad (Fig. 7) (Wang W. et al., 2016). Notably, the K88E substitution significantly reduced membrane fusion efficiency, suggesting that the charged residue K88 plays an important role in GPC-mediated membrane fusion, which might sense the acidic pH within the endolysosomal compartment, thus promoting receptor switch and the conformational change of $GP1_{LASV}$. Thus, we infer that maximal LAMP1 binding and membrane fusion of LASV require a positive charge at position 88 in GPC_{LASV}. The mechanism involving K88 might be similar to that of K33, a key charged residue located in the putative membrane-proximal region of the SSP. It has been reported that charge-changing substitutions of K33 affect the maturation of GPC and its downstream function; thus, the K33 residue is crucial for GPC sensitivity to pH (York and Nunberg, 2006). Another positively charged residue, H170, is located on the top of the $GP1_{LASV}$ structure and may function similarly to K88 and K33 in sensing pH. Moreover, L84 and L107 are located in the vicinity of the histidine triad and may be important for maintaining the structure of the histidine triad and the $GP1_{LASV}$-LAMP1 interaction interface. However, neither L105 nor H115 conforms to the above characteristics, we considered them to be less important than the four amino acids above in terms of structure, thus we didn't choose L105 and H115 in the further study. Interestingly, mutations T87S and V164I significantly increased binding of GP1-Fc to LAMP1, it is very meaningful to investigate the effect of T87S and V164I mutations on LASV entry, replication, infectivity, growth curve, and tropism in the future. We proposed that T87S and V164I mutations maybe change the structure or stability of GP1-Fc, resulting in the binding activity of GP1-Fc to LAMP1 significantly increased.

LASV GPC is a heavily glycosylation-modified protein containing 11N-glycosylation sites (Asn-X-Thr/Ser, where X is any amino acid except proline), seven of which are located in GP1 and four in GP2. All N-linked glycan chains paly critical roles in GPC cleavage, folding, receptor binding, membrane fusion, and immune evasion. By using NetNGlyc

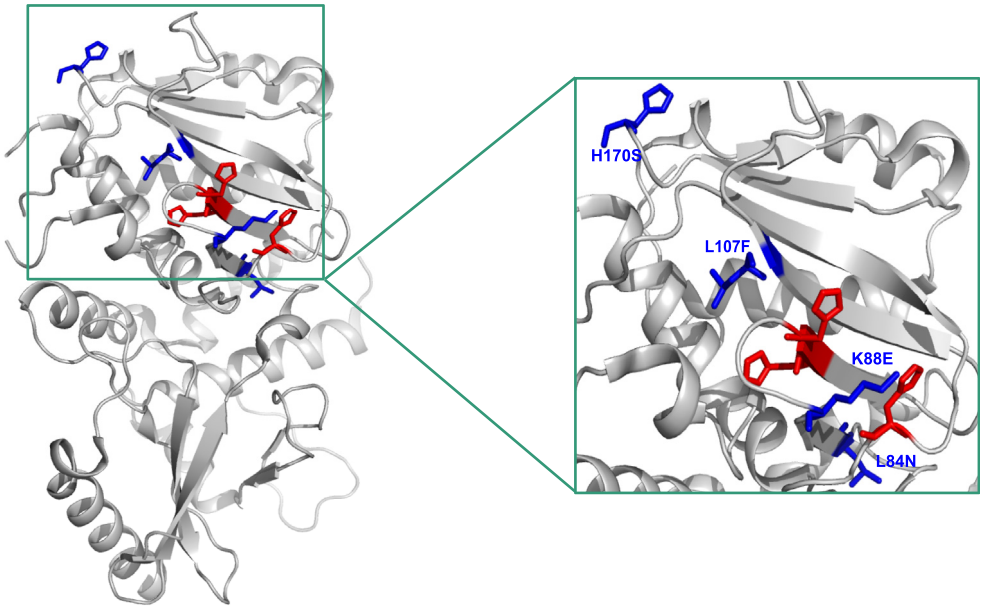

Fig. 7. Crystal structure of $GP1_{LASV}$ (PDB: 5VK2), showing the positions L84, K88, L107, H170 (blue) and the histidine triad (red); these residues are magnified in the inset box.

server, the study evaluated the molecular interactions between the LASV GPC trimeric complex and the human LAMP1, mediated by the predicted N-linked glycosylated amino residues (Chukwudozie, 2020). From the prediction of the N-GlcNAc residues of the GP1, at position 89 of the asparagine sequons, it was predicted as the only negative glycosite, which was lower than the threshold value of 0.5, while other asparagine positions and sequences succeeding it were confirmed as positive glycosites, as they exceeded 0.5. These glycosylated residues mediate the LASV interaction with human LAMP1. Additionally, our group recently focused on the first glycosylation site (N79) due to its deletion mutant (N79Q) results in an enhanced membrane fusion, whereas it exhibits little effect on GPC expression, cleavage, and receptor binding. Moreover, the pseudotype virus bearing GPC_{N79Q} was more sensitive to the neutralizing antibody 37.7H and was attenuated in virulence (Dong et al., 2023).

To investigate whether these substitutions affect the binding of $GP1_{LCMV}$ to LAMP1, we constructed four $GP1_{LCMV}$ mutant expression plasmids (N90L, V94K, F110L, and S174H, according to the residues in GPC_{LCMV}). However, none of these $GP1_{LCMV}$ mutants interacted with LAMP1 (Data was not been published). This suggests that the impact of these four residues in $GP1_{LASV}$ was greater than that in $GP1_{LCMV}$, and that the corresponding mutations in $GP1_{LCMV}$ were not sufficient to promote its interaction with LAMP1.

To date, there is no published structure of LAMP1 co-crystallized with $GP1_{LASV}$; therefore, we performed a BLI assay to evaluate the binding of distal-LAMP1 and $GP1_{LASV}$. Distal-LAMP1 refers to residues 27–194 of LAMP1, the key domain that partially reflects the physiological state and function of LAMP1 in cells; thus, it has been used to study LAMP1 function (Li et al., 2016). The data from this assay were consistent with the pulldown assay, as distal-LAMP1 plays a critical role in LAMP1 binding.

LAMP1 triggers significant increase in GPC_{LASV} spike complex-mediated cell entry (Israeli et al., 2017). However, we found that LASV infection was not completely inhibited in LAMP1-knockout A549 cells (Fig. 5B). These data are consistent with those from a previous study, in which the infectivity of LASV VSV pseudoviruses was reduced by 70%–85% in LAMP1-knockout cells relative to wild-type cells (Hulseberg et al., 2018). Based on the results of our study, preliminary determination of the LAMP1 and LASV-GP1 interaction interface from a structural perspective and mutation of the amino acid site of LAMP1 at this interface will help to precisely understand the mechanism of LAMP1-GP1 interaction. As LAMP1 is a protein on the lysosomal membrane and widely distributed in most human tissues, sequencing LAMP1 in Lassa fever patients in areas where Lassa fever transmission is endemic is of scientific significance. The sequencing of LAMP1 in the infected population with different sex, age, disease level and prognosis, with special emphasis on areas with high serological positivity and individuals with special disease, such as immune survivors and infants born to pregnant women with Lassa fever, will help to investigate whether there are mutations or key amino acid sites in LAMP1, which will help to clarify the virus transmission pattern and population immunity. This will help to clarify the virus transmission pattern and population immune effect.

These four residues, identified as being involved in LASV glycoprotein receptor switch, are significant for understanding the mechanism underlying host-pathogen interactions and provide new insights for further study of invasive mechanisms, and therefore potential inhibitors, of LASV. Further elucidation of the relationship between α-DG and LAMP1 and characterization of the LAMP1-GP1 interaction will clarify the events that occur during LASV infection and facilitate specific strategies to clinically inhibit this crucial interaction (Shimojima et al., 2012).

5. Conclusion

In this study, we identified four residues in LASV GP1 protein, L84, K88, L107, and H170, were critical for receptor switch. Substituting any of the four residues with the corresponding LCMV residues (L84 N, K88E, L10F, and H170S) reduced the binding affinity of LASV GP1 for LAMP1. The discovery of four previously unknown residues holds significant reference value for further exploration of the receptor switching mechanism, immune escape, and the development of anti-LASV infection drugs.

Data availability

All the data generated during the current study are included in the manuscript. The raw data supporting the conclusions of this article will be made available by the authors, without undue reservation.

Ethics statement

This article does not contain any studies with human or animal subjects performed by any of the authors.

Author contributions

Conceptualization, W.W. and J.G.; methodology, W.W., J.G., W.Y., X.J., Y.L., and S.D.; validation, J.G., W.Y., X.J., Y.L., and S.D.; investigation, W.W., J.G., X.J., Y.L., S.D., and G.X.; writing – original draft preparation, W.W. and J.G.; writing – review and editing, W.W., J.G. and W.Y.; supervision, W.W.; project administration, W.W. and J.G.; and funding acquisition, W.W. and J.G. All authors have read and agreed to the published version of the manuscript. All authors have read and agreed to the published version of the manuscript.

Conflict of interest

The authors declare no conflict of interest.

Acknowledgements

We thank Professor Ron Diskin (Department of Structural Biology, Weizmann Institute of Science, Rehovot, Israel) for providing technical details and plasmids. We thank the Center for Instrumental Analysis and Metrology, and Institutional Center for Shared Technologies and Facilities of Wuhan Institute of Virology, CAS, for providing technical assistance. This work was supported by the National Key Research and Development Program of China (2023YFC2605504, 2022YFC2303300), the National Natural Sciences Foundation of China (82172273 and 31670165), the Open Research Fund Program of the State Key Laboratory of Virology of China (2023JZZD-01), the Health research project of Shaanxi Province (2022D040), the Science and Technology Planning Project of Shaanxi Provincial Education Department (22JK0545), and the Natural Science Basic Research Program of Shaanxi (2024JC-YBQN-0922).

References

Acciani, M., Alston, J.T., Zhao, G., Reynolds, H., Ali, A.M., Xu, B., Brindley, M.A., 2017. Mutational analysis of Lassa virus glycoprotein highlights regions required for alpha-dystroglycan utilization. J. Virol. 91 e00574–17.

Cao, J., Zhang, G., Zhou, M., Liu, Y., Xiao, G., Wang, W., 2021. Characterizing the Lassa virus envelope glycoprotein membrane proximal external region for its role in fusogenicity. Virol. Sin. 36, 273–280.

Carette, J.E., Raaben, M., Wong, A.C., Herbert, A.S., Obernosterer, G., Mulherkar, N., Kuehne, A.I., Kranzusch, P.J., Griffin, A.M., Ruthel, G., Cin, P.D., Dye, J.M., Whelan, S.P., Chandran, K., Brummelkamp, T.R., 2011. Ebola virus entry requires the cholesterol transporter Niemann–Pick C1. Nature 477, 340–343.

Chukwudozie, O.S., 2020. The function annotations of ST3GAL4 in human lamp1 and lassa virus GP-C interaction from the perspective of systems virology. Access Microbiol 2, acmi000146.

Cohen-Dvashi, H., Kilimnik, I., Diskin, R., 2018. Structural basis for receptor recognition by Lujo virus. Nat Microbiol 3, 1153–1160.

Cohen-Dvashi, H., Cohen, N., Israeli, H., Diskin, R., 2015. Molecular mechanism for LAMP1 recognition by Lassa virus. J. Virol. 89, 7584–7592.

Cohen-Dvashi, H., Israeli, H., Shani, O., Katz, A., Diskin, R., 2016. Role of LAMP1 binding and ph sensing by the spike complex of Lassa virus. J. Virol. 90, 10329–10338.
Dong, S., Mao, W., Liu, Y., Jia, X., Zhang, Y., Zhou, M., Hou, Y., Xiao, G., Wang, W., 2023. Deletion of the first glycosylation site promotes Lassa virus glycoprotein-mediated membrane fusion. Virol. Sin. 38, 380–386.
Enria, D.A., Briggiler, A.M., Fernandez, N.J., Levis, S.C., Maiztegui, J.I., 1984. Importance of dose of neutralising antibodies in treatment of argentine haemorrhagic fever with immune plasma. Lancet 2, 255–256.
Goeijenbier, M., Wagenaar, J., Goris, M., Martina, B., Henttonen, H., Vaheri, A., Reusken, C., Hartskeerl, R., Osterhaus, A., Van Gorp, E., 2013. Rodent-borne hemorrhagic fevers: under-recognized, widely spread and preventable- epidemiology, diagnostics and treatment. Crit. Rev. Microbiol. 39, 26–42.
Hulseberg, C.E., Fénéant, L., Szymańska, K.M., White, J.M., 2018. LAMP1 increases the efficiency of Lassa virus infection by promoting fusion in less acidic endosomal compartments. mBio 9, e01818, 17.
Israeli, H., Cohen-Dvashi, H., Shulman, A., Shimon, A., Diskin, R., 2017. Mapping of the Lassa virus LAMP1 binding site reveals unique determinants not shared by other old world arenaviruses. PLoS Pathog. 13, e1006337.
Jae, L.T., Brummelkamp, T.R., 2015. Emerging intracellular receptors for hemorrhagic fever viruses. Trends Microbiol. 23, 392–400.
Jae, L.T., Raaben, M., Herbert, A.S., Kuehne, A.I., Wirchnianski, A.S., Soh, T.K., Stubbs, S.H., Janssen, H., Damme, M., Saftig, P., Whelan, S.P., Dye, J.M., Brummelkamp, T.R., 2014. Virus entry. Lassa virus entry requires a trigger-induced receptor switch. Science 344, 1506–1510.
Kumar, S., Sarkar, A., 2019. Capturing the inherent structural dynamics of the HIV-1 envelope glycoprotein fusion peptide. Nat. Commun. 10, 763.
Li, S., Sun, Z., Pryce, R., Parsy, M.L., Fehling, S.K., Schlie, K., Siebert, C.A., Garten, W., Bowden, T.A., Strecker, T., Huiskonen, J.T., 2016. Acidic pH-induced conformations and LAMP1 binding of the Lassa virus glycoprotein spike. PLoS Pathog. 12, e1005418.
Liu, Y., Guo, J., Cao, J., Zhang, G., Jia, X., Wang, P., Xiao, G., Wang, W., 2021. Screening of botanical drugs against Lassa virus entry. J. Virol. 95, e02429, 20.
Moraz, M.L., Pythoud, C., Turk, R., Rothenberger, S., Pasquato, A., Campbell, K.P., Kunz, S., 2013. Cell entry of Lassa virus induces tyrosine phosphorylation of dystroglycan. Cell Microbiol. 15, 689–700.
Nunberg, J.H., York, J., 2012. The curious case of arenavirus entry, and its inhibition. Viruses 4, 83–101.
Oppliger, J., Torriani, G., Herrador, A., Kunz, S., 2016. Lassa virus cell entry via dystroglycan involves an unusual pathway of macropinocytosis. J. Virol. 90, 6412–6429.
Raaben, M., Jae, L.T., Herbert, A.S., Kuehne, A.I., Stubbs, S.H., Chou, Y.Y., Blomen, V.A., Kirchhausen, T., Dye, J.M., Brummelkamp, T.R., Whelan, S.P., 2017. NRP2 and CD63 are host factors for lujo virus cell entry. Cell Host Microbe 22, 688–696 e685.
Radoshitzky, S.R., Bao, Y., Buchmeier, M.J., Charrel, R.N., Clawson, A.N., Clegg, C.S., DeRisi, J.L., Emonet, S., Gonzalez, J.P., Kuhn, J.H., Lukashevich, I.S., Peters, C.J., Romanowski, V., Salvato, M.S., Stenglein, M.D., de la Torre, J.C., 2015. Past, present, and future of arenavirus taxonomy. Arch. Virol. 160, 1851–1874.
Sanchez, A., Pifat, D.Y., Kenyon, R.H., Peters, C.J., McCormick, J.B., Kiley, M.P., 1989. Junin virus monoclonal antibodies: characterization and cross-reactivity with other arenaviruses. J. Gen. Virol. 70, 1125–1132.
Shimojima, M., Stroher, U., Ebihara, H., Feldmann, H., Kawaoka, Y., 2012. Identification of cell surface molecules involved in dystroglycan-independent Lassa virus cell entry. J. Virol. 86, 2067–2078.
Thomson, E.C., Rosen, L.E., Shepherd, J.G., Spreafico, R., da Silva Filipe, A., Wojcechowskyj, J.A., Davis, C., Piccoli, L., Pascall, D.J., Dillen, J., Lytras, S., Czudnochowski, N., Shah, R., Meury, M., Jesudason, N., De Marco, A., Li, K., Bassi, J., O'Toole, A., Pinto, D., Colquhoun, R.M., Culap, K., Jackson, B., Zatta, F., Rambaut, A., Jaconi, S., Sreenu, V.B., Nix, J., Zhang, I., Jarrett, R.F., Glass, W.G., Beltramello, M., Nomikou, K., Pizzuto, M., Tong, L., Cameroni, E., Croll, T.I., Johnson, N., Di Iulio, J., Wickenhagen, A., Ceschi, A., Harbison, A.M., Mair, D., Ferrari, P., Smollett, K., Sallusto, F., Carmichael, S., Garzoni, C., Nichols, J., Galli, M., Hughes, J., Riva, A., Ho, A., Schiuma, M., Semple, M.G., Openshaw, P.J.M., Fadda, E., Baillie, J.K., Chodera, J.D., Rihn, S.J., Lycett, S.J., Virgin, H.W., Telenti, A., Corti, D., Robertson, D.L., Snell, G., 2021. Circulating SARS-CoV-2 spike N439K variants maintain fitness while evading antibody-mediated immunity. Cell 184, 1171–1187.e1120.
Wang, H., Shi, Y., Song, J., Qi, J., Lu, G., Yan, J., Gao, G.F., 2016. Ebola viral glycoprotein bound to its endosomal receptor Niemann-Pick C1. Cell 164, 258–268.
Wang, P., Liu, Y., Zhang, G., Wang, S., Guo, J., Cao, J., Jia, X., Zhang, L., Xiao, G., Wang, W., 2018. Screening and identification of Lassa virus entry inhibitors from an FDA-approved drug library. J. Virol. 92, e00954, 18.
Wang, W., Zhou, Z., Zhang, L., Wang, S., Xiao, G., 2016. Structure-function relationship of the mammarenavirus envelope glycoprotein. Virol. Sin. 31, 380–394.
York, J., Nunberg, J.H., 2006. Role of the stable signal peptide of Junin arenavirus envelope glycoprotein in pH-dependent membrane fusion. J. Virol. 80, 7775–7780.
Yun, N.E., Walker, D.H., 2012. Pathogenesis of lassa fever. Viruses 4, 2031–2048.
Zhu, X., Liu, Y., Guo, J., Cao, J., Wang, Z., Xiao, G., Wang, W., 2021. Effects of N-linked glycan on Lassa virus envelope glycoprotein cleavage, infectivity, and immune response. Virol. Sin. 36, 774–783.